Rotation-Induced Microscopic Binding and the Emergence of a Contracting Rod

A Finite-Stiffness Effective Theory with a Microscopic Mediator Model, Quantitative Thresholds, and Experimental Controls

S. M. H. Emamifar

Independent Research Collaboration on
Black Hole and Cosmology Concepts (IRCBHC)

ORCID: 0009-0007-6257-0163

July 2026

Abstract

A rotating extended body is ordinarily expected to develop outward centrifugal strain. This expectation presumes that the microscopic equilibrium structure of the material is independent of the rotational state. The present paper studies a different conditional possibility: bulk rotation may couple to an internal phase or activity variable of the constituents, and the resulting change of internal state may strengthen their binding strongly enough to reduce their preferred separation. In that regime, the material can become shorter and stiffer as its angular velocity increases, despite the simultaneous outward centrifugal tendency.

The analysis begins with the rod and spinning-top thought experiment. A rod transmits the inward force required for circular motion, but the rod itself is usually treated as primitive. Here the direction of explanation is reversed: the rod is derived as a coarse-grained network of microscopic bonds. A covariant finite-stiffness sector couples a scalar internal rate to the magnitude of material vorticity and contains the earlier strong-locking relation as a controlled limiting branch. To reduce the arbitrariness of the binding hypothesis, a microscopic mediator toy model is introduced: integrating out a stable scalar mediator produces an attractive amplitude that increases with the internal rate in an explicit parameter domain. A general repulsive-attractive pair potential is then analyzed using this induced amplitude. Two conditional theorems follow. First, the equilibrium bond separation decreases with the magnitude of bulk rotation. Second, the local bond stiffness and the coarse-grained elastic modulus increase with rotation.

For a closed ring, the microscopic preferred circumference becomes rotation dependent. Combining this dependence with the local relativistic relation between laboratory circumference and summed comoving length yields the generalized exact branch

$$r(\Omega) = \frac{\rho_\star(\Omega)}{\sqrt{1 + \Omega^2 \rho_\star^2(\Omega)/c^2}},$$

where $\rho_\star(\Omega)$ is the preferred proper radius generated by the microscopic binding sector. If $\rho'_\star(\Omega) \le 0$, the laboratory radius decreases monotonically. The tangential speed remains subluminal for every finite Ω and finite $\rho_\star$.

The paper also formulates an observer-scale independence lemma: changing the size or resolution of a passive observer changes the measurement map and available effective description, not the physical state of the observed system. This clarifies why a macroscopically continuous rod may consistently be represented microscopically as a sparse dynamical network without making the physical truth dependent on the observer's size.

The model does not establish that ordinary matter possesses the proposed rotation-phase coupling, and it does not derive a universal external gravitational field. It now provides, however, a positive finite-stiffness stationary completion, an explicit mediator mechanism for the sign of the induced attraction, dimensionless competition criteria, illustrative laboratory-scale thresholds, a thermal and mechanical systematics budget, and correlated observables by which the effective coefficients can be bounded or falsified.

Keywords: rotation-induced binding; phase locking; contracting rod; radial accommodation; relativistic elasticity

Contents

1 Introduction

The ordinary macroscopic picture of a spinning object is simple. The distinction between relativistic rigidity, rotational motion, and material deformation has a long history beginning with Born and Ehrenfest [3, 4] and continuing in relativistic treatments of rotating systems [10, 6]. A material element at radius r has tangential speed

$$v = \Omega r, \tag{1}$$

and requires inward acceleration

$$a_{\mathrm{c}} = \Omega^2 r \tag{2}$$

in the nonrelativistic limit. In the corotating description, the same equilibrium is represented by an outward centrifugal inertial term balanced by inward stresses or constraints.

This familiar reasoning normally assumes that the constitutive properties of the material are fixed while the rotational load is increased. Under that assumption, larger rotation produces larger tensile stress and usually outward deformation. The assumption is physically reasonable for ordinary engineering materials over ordinary ranges of angular velocity, but it is not a theorem of kinematics or relativity. A microscopic interaction law could, in principle, depend on the rotational state of the material. If that dependence strengthens the attractive part of the binding more rapidly than centrifugal loading stretches the body, the sign of the net deformation can reverse.

The central question of this work is therefore:

> Can an increase of bulk rotation alter a microscopic internal state in such a way that the preferred separation of material constituents decreases and the resulting coarse-grained structure becomes simultaneously shorter and stiffer?

The paper answers this question conditionally. It does not assume that every rotating material behaves this way. Instead, it identifies a minimal set of mathematical conditions under which the conclusion follows, derives the consequences of those conditions, and separates those deductions from the empirical hypothesis that real matter realizes the required coupling.

The conceptual starting point is the rod and spinning-top thought experiment [12]. A rotating rod can transmit the inward force needed to hold a mass on a circular path. This shows that circular kinematics do not uniquely reveal the mechanism that produces them. The present work pushes the thought experiment one level deeper. Rather than accepting the rod as a primitive rigid object, it asks what microscopic dynamics could make a rod emerge, and what happens if those dynamics are themselves rotation dependent.

The second starting point is radial accommodation in a rotating ring. If a closed ring preserves a preferred summed comoving circumference while its laboratory tangential elements obey the local Lorentz relation, its laboratory radius satisfies a self-consistent contraction map [11]. The present model generalizes that construction: the preferred comoving circumference is no longer assumed constant, but is derived from a rotation-dependent microscopic bond length.

The main results are:

(i) a covariant strong-locking relation between material vorticity and an internal activity rate;

(ii) a contraction theorem for the microscopic equilibrium separation;

(iii) a stiffening theorem for the microscopic bond and the macroscopic elastic modulus;

(iv) an emergent-rod construction obtained by coarse graining a chain of such bonds;

(v) a generalized exact radial-accommodation branch for a closed ring;

(vi) a low-rotation expansion that produces explicit quadratic signatures;

(vii) a clear separation between internal structural attraction, equivalent inward acceleration, and a genuine external gravitational field.

2 Claim Status and Scope

The argument contains deductions, assumptions, interpretations, and open problems. They are not interchangeable. Table 1 records the status of the principal statements.

Table 1: Logical status of the principal statements.

Status	Statement
Derived	Circular motion maintained by a rod requires an inward transmitted force with magnitude $m\Omega^2 r$ in the nonrelativistic limit.
Derived	For the specified pair potential, the equilibrium separation and local curvature can be calculated exactly.
Conditional theorem	If the attractive amplitude increases with an internal activity rate, and that rate increases with rotational vorticity, the equilibrium separation decreases with rotation.
Conditional theorem	Under the same assumptions, the microscopic stiffness and coarse-grained modulus increase with rotation.
Conditional theorem	If a closed ring adopts the rotation-dependent preferred proper circumference, the generalized radial map follows exactly.
Model assumption	The internal phase/activity sector is coupled to material vorticity through a positive finite-stiffness potential; the strong-locking relation is its large-stiffness stationary limit.
Physical hypothesis	Some microscopic constituents or collective modes of real matter realize the mediator and vorticity couplings with parameters large enough to compete with ordinary centrifugal strain.
Open problem	A derivation of the effective coefficients from a specified material or fundamental theory, a complete relativistic continuum Hamiltonian, and a universal external-field completion.

The paper is therefore neither a purely verbal analogy nor a completed fundamental theory. It is a conditional effective theory with explicit theorems and a precisely identified empirical gap.

3 The Rod and Spinning-Top Inverse Problem

3.1 Two ways to obtain circular motion

For a test mass moving in a circular Newtonian gravitational orbit around a central mass M,

$$\frac{v^2}{r} = \frac{GM}{r^2}, \tag{3}$$

so that

$$v_{\rm grav}(r) = \sqrt{\frac{GM}{r}}, \qquad \Omega_{\rm grav}(r) = \sqrt{\frac{GM}{r^3}}. \tag{4}$$

For a point rigidly constrained to participate in a rotating structure,

$$v_{\rm rod}(r) = \Omega r, \tag{5}$$

and the inward force transmitted by the constraint is

$$\boxed{F_{\rm rod} = m\Omega^2 r.} \tag{6}$$

At one selected radius, choosing $\Omega^2 = GM/r^3$ makes the two systems share the same instantaneous speed and radial acceleration. Across many radii, however, a rigid common Ω and a Keplerian $\Omega \propto r^{-3/2}$ are different dynamical organizations.

The general lesson is the non-uniqueness of the inverse map

$$\boldsymbol{x}(t) \longrightarrow \text{physical mechanism.} \tag{7}$$

A trajectory determines velocity and acceleration, but an acceleration may be supplied by gravity, a mechanical constraint, electromagnetic interaction, pressure gradients, or another stress-transmission architecture.

3.2 The reversal of the explanatory direction

In the usual rod model, the rod is given and the transmitted force is calculated. The present work reverses the order:

$$\begin{aligned} \text{microscopic interactions} &\longrightarrow \text{coherent material network} \\ &\longrightarrow \text{effective rod} \longrightarrow \text{transmitted inward force.} \end{aligned} \tag{8}$$

The important question is no longer only how a rod holds an external mass. It is how the constituents of the rod hold one another, and whether their binding law can change when the complete structure rotates.

3.3 Equivalent inward acceleration is not yet gravity

The inward acceleration associated with the constraint can be assigned an equivalent Newtonian mass profile,

$$M_{\text{eq}}(r) = \frac{r^3\Omega^2(r)}{G} = \frac{rv^2(r)}{G}. \tag{9}$$

This is a kinematic dictionary. It says which Newtonian mass profile would produce the same radial acceleration. It does not prove that the rotating structure generates an external gravitational field, nor that a free test body outside the material is attracted according to equation (9).

This distinction will remain explicit throughout the paper:

$$\boxed{\text{internal constraint attraction} \neq \text{universal external gravity.}} \tag{10}$$

4 Observer-Scale Independence of Physical Structure

The microscopic picture is often rejected intuitively because a solid rod appears continuous and an atom does not appear as a visible mechanical system. This objection mixes physical structure with observational resolution. The following lemma makes the distinction precise.

Definition 4.1 (Physical state and measurement map)**.** Let the physical state of a system be represented schematically by

$$\mathcal{S} = \{g_{\mu\nu}, T_{\mu\nu}, \Psi_A, X_I^\mu, \ldots\}, \tag{11}$$

where the collection may contain geometry, matter fields, phase variables, material worldlines, and stresses. An observer with characteristic size ℓ_{obs} and resolution $\delta\ell$ produces data through a measurement map

$$\mathcal{D}_{\text{obs}} = \mathcal{M}_{\ell_{\text{obs}},\delta\ell}[\mathcal{S}]. \tag{12}$$

Lemma 4.2 (Observer-scale independence)**.** *Suppose that $\mathcal{S}$ satisfies equations of motion*

$$\mathcal{E}[\mathcal{S}] = 0 \tag{13}$$

with specified sources and boundary conditions. Consider two passive observers whose backreaction on the system is negligible. Changing the observers' characteristic sizes or resolutions may change their measurement maps, but it does not change the physical solution $\mathcal{S}$.

Proof. By assumption, the observer is passive and its size is not a source or boundary datum in $\mathcal{E}[\mathcal{S}] = 0$. Replacing one passive measurement map by another changes

$$\mathcal{M}_1[\mathcal{S}] \longrightarrow \mathcal{M}_2[\mathcal{S}], \tag{14}$$

but leaves the equation and its physical solution unchanged. Thus the records may differ while the underlying state does not. □

Symbolically,

$$\ell_{\text{obs}} \to \lambda \ell_{\text{obs}} \quad \Rightarrow \quad \mathcal{M} \to \mathcal{M}', \qquad \text{not} \qquad \mathcal{S} \to \mathcal{S}'. \tag{15}$$

This lemma is not a claim of dynamical scale invariance. Physically rescaling a system changes its parameters. For example, at fixed $\beta = v/c$,

$$a_{\text{c}} = \frac{\beta^2 c^2}{r} \tag{16}$$

changes when the system radius changes. Observer-scale independence means only that making the observer smaller does not, by itself, transform the system into a different physical system.

A hypothetical microscopic observer could resolve the rod as a network of separated constituents, phase correlations, and interaction gradients. A macroscopic observer describes the same state through density, stress, and elastic modulus. These are different effective descriptions of one organization:

$$\boxed{\text{coarse-grained continuous rod} \longleftrightarrow \text{resolved microscopic network.}} \tag{17}$$

The analogy does not require an atom to be a classical miniature Solar System. It requires only that the microscopic theory possess resolvable degrees of freedom whose coarse-grained collective behavior is material rigidity.

5 Kinematic and Microscopic Variables

5.1 Material four-velocity and vorticity

Let u^μ be the material four-velocity,

$$u^\mu u_\mu = -c^2. \tag{18}$$

The projector into the instantaneous local rest space is

$$h_{\mu\nu} = g_{\mu\nu} + \frac{u_\mu u_\nu}{c^2}. \tag{19}$$

The projected vorticity tensor is

$$\omega_{\mu\nu} = h_\mu{}^\alpha h_\nu{}^\beta \nabla_{[\alpha} u_{\beta]}. \tag{20}$$

Define the nonnegative scalar magnitude

$$\varpi^2 \equiv \frac{1}{2}\omega_{\mu\nu}\omega^{\mu\nu}. \tag{21}$$

For weakly relativistic, nearly rigid rotation, ϖ is proportional to the ordinary angular speed $|\Omega|$, with a convention-dependent numerical factor that may be absorbed into a coupling coefficient.

5.2 Internal phase and activity rate

Associate with each microscopic constituent, or with a coarse-grained material cell, an internal phase

$$\Xi = A_{\Xi}\mathrm{e}^{\mathrm{i}\Theta}. \tag{22}$$

The comoving phase rate is

$$s \equiv u^{\mu}\nabla_{\mu}\Theta. \tag{23}$$

The variable s is an internal activity rate measured with respect to the material proper time. It is not automatically identical to an electron's classical orbital frequency, and the model does not require a Bohr-orbit interpretation.

5.3 Parity-even finite-stiffness locking sector

A minimal orientation-independent coupling should depend on the magnitude of rotation rather than the sign of Ω. Introduce a positive internal activity variable σ and define

$$S^2(\varpi) \equiv \sigma_0^2 + \chi^2\varpi^2, \tag{24}$$

where $\sigma_0 > 0$ and χ is a coupling coefficient. Instead of imposing $\sigma = S$ as a primitive constraint, assign the positive stationary energy density

$$U_{\mathrm{lock}}(\sigma, \varpi) = \frac{K_\sigma}{4}\left[\sigma^2 - S^2(\varpi)\right]^2, \qquad K_\sigma > 0. \tag{25}$$

Its stationary branches satisfy

$$\frac{\partial U_{\mathrm{lock}}}{\partial \sigma} = K_\sigma \sigma \left[\sigma^2 - S^2(\varpi)\right] = 0. \tag{26}$$

On the positive-activity branch,

$$\boxed{\sigma_\star(\varpi) = \sqrt{\sigma_0^2 + \chi^2\varpi^2}.} \tag{27}$$

This relation is therefore an equilibrium result of a bounded-below potential, not a holonomic constraint inserted without an energy cost. The curvature at the positive minimum is

$$m_\sigma^2(\varpi) \equiv \left.\frac{\partial^2 U_{\mathrm{lock}}}{\partial \sigma^2}\right|_{\sigma_\star} = 2K_\sigma \sigma_\star^2 > 0, \tag{28}$$

so homogeneous activity perturbations are locally stable.

To connect the activity variable to a comoving phase Θ, introduce a second positive penalty,

$$U_\Theta = \frac{K_\Theta}{2}\left(u^\mu \nabla_\mu \Theta - \sigma\right)^2, \qquad K_\Theta > 0. \tag{29}$$

The large-K_Θ limit gives $u^\mu \nabla_\mu \Theta \simeq \sigma$. A reduced homogeneous Hamiltonian for the independent activity mode can be chosen as

$$H_\sigma = \frac{p_\sigma^2}{2I_\sigma} + U_{\rm lock}(\sigma, \varpi), \qquad I_\sigma > 0, \tag{30}$$

which is manifestly bounded below. This closes the most immediate stationary stability gap, while a complete relativistic continuum Hamiltonian including the phase, strain, and vorticity sectors remains an open problem.

For a stationary rotating configuration in which $\varpi = \zeta|\Omega|$,

$$\sigma_\star(\Omega) = \sqrt{\sigma_0^2 + \chi^2\zeta^2\Omega^2}, \tag{31}$$

and hence

$$\frac{d\sigma_\star}{d|\Omega|} = \frac{\chi^2\zeta^2|\Omega|}{\sigma_\star} > 0 \qquad (|\Omega| > 0). \tag{32}$$

This is the first link in the proposed causal chain.

6 Rotation-Dependent Microscopic Binding

6.1 A microscopic mediator toy model for $A'(\sigma) > 0$

The monotonicity of the attractive amplitude need not be postulated without an example. Consider a stable scalar mediator ϕ coupled to a separation-dependent source $J(d)$, with local energy

$$U_\phi = \frac{1}{2}M_\phi^2(\sigma)\phi^2 + \frac{\lambda_\phi}{4}\phi^4 - J(d)\phi, \qquad \lambda_\phi \geq 0, \tag{33}$$

where

$$M_\phi^2(\sigma) = M_0^2 - g_\sigma\left(\sigma^2 - \sigma_0^2\right), \qquad g_\sigma > 0. \tag{34}$$

In the weak-source, Gaussian regime, with $M_\phi^2(\sigma) > 0$, minimizing over ϕ gives

$$\phi_\star \simeq \frac{J(d)}{M_\phi^2(\sigma)}, \tag{35}$$

and the induced interaction is

$$U_{\rm ind}(d, \sigma) \simeq -\frac{J^2(d)}{2M_\phi^2(\sigma)}. \tag{36}$$

If $J^2(d) \propto (d_\star/d)^n$, the attractive amplitude is

$$\boxed{A(\sigma) = \frac{A_J}{M_\phi^2(\sigma)}, \qquad A_J > 0.} \tag{37}$$

Inside the stable domain $M_\phi^2(\sigma) > 0$,

$$\boxed{A'(\sigma) = \frac{2A_J g_\sigma \sigma}{\left[M_\phi^2(\sigma)\right]^2} > 0 \qquad (\sigma > 0).} \tag{38}$$

Thus the required sign occurs in an explicit, bounded parameter domain of an ordinary mediator model. This does not identify the mediator of a real material, but it converts the sign condition from a purely free assumption into a realizable effective mechanism. The approximation fails as $M_\phi^2 \to 0$; the quartic term and fluctuations must then be retained.

6.2 A general pair potential

Let d be the proper separation of neighboring constituents. Consider the effective pair energy

$$U(d, \sigma) = B\left(\frac{d_\star}{d}\right)^m - A(\sigma)\left(\frac{d_\star}{d}\right)^n, \qquad m > n > 0, \tag{39}$$

where $B > 0$, $d_\star > 0$, and $A(\sigma) > 0$. The first term supplies a short-range repulsive core; the second supplies attraction.

The essential microscopic hypothesis is

$$\boxed{A'(\sigma) > 0.} \tag{40}$$

Thus larger internal activity strengthens the attractive amplitude. The model remains agnostic about whether the underlying origin is electromagnetic, phase-gradient, topological, or another microscopic sector.

6.3 Exact equilibrium separation

The stationary separation satisfies

$$\frac{\partial U}{\partial d} = 0. \tag{41}$$

Using equation (39),

$$-mB\frac{d_\star^m}{d^{m+1}} + nA(\sigma)\frac{d_\star^n}{d^{n+1}} = 0. \tag{42}$$

Therefore,

$$\boxed{d_{\rm eq}(\sigma) = d_\star\left[\frac{mB}{nA(\sigma)}\right]^{1/(m-n)}.} \tag{43}$$

Theorem 6.1 (Microscopic contraction theorem)**.** *Assume* $m > n > 0$, $A(\sigma) > 0$, $A'(\sigma) > 0$, *and* $\mathrm{d}\sigma/\mathrm{d}|\Omega| > 0$. *Then*

$$\frac{\mathrm{d}d_{\mathrm{eq}}}{\mathrm{d}|\Omega|} < 0. \tag{44}$$

Proof. Taking the logarithmic derivative of equation (43) gives

$$\frac{1}{d_{\mathrm{eq}}}\frac{\mathrm{d}d_{\mathrm{eq}}}{\mathrm{d}|\Omega|} = -\frac{1}{m-n}\frac{A'(\sigma)}{A(\sigma)}\frac{\mathrm{d}\sigma}{\mathrm{d}|\Omega|}. \tag{45}$$

Every factor on the right-hand side except the leading minus sign is positive. The result follows. □

This theorem is a genuine logical consequence of the model assumptions. It does not require an appeal to observer size or visual analogy.

6.4 Exact bond stiffness

The local stiffness is the curvature at equilibrium,

$$k_b(\sigma) \equiv \left.\frac{\partial^2 U}{\partial d^2}\right|_{d=d_{\mathrm{eq}}}. \tag{46}$$

Using the equilibrium relation to simplify the second derivative yields

$$\boxed{k_b(\sigma) = \frac{n(m-n)A(\sigma)}{d_\star^2}\left[\frac{nA(\sigma)}{mB}\right]^{(n+2)/(m-n)}.} \tag{47}$$

Equivalently,

$$k_b \propto A^{(m+2)/(m-n)}. \tag{48}$$

Theorem 6.2 (Microscopic stiffening theorem)**.** *Under the assumptions of the microscopic contraction theorem,*

$$\frac{\mathrm{d}k_b}{\mathrm{d}|\Omega|} > 0. \tag{49}$$

Proof. From equation (48),

$$\frac{1}{k_b}\frac{\mathrm{d}k_b}{\mathrm{d}|\Omega|} = \frac{m+2}{m-n}\frac{A'(\sigma)}{A(\sigma)}\frac{\mathrm{d}\sigma}{\mathrm{d}|\Omega|} > 0. \tag{50}$$

□

The same change of microscopic state therefore produces two effects at once:

$$\boxed{|\Omega|\uparrow \implies d_{\mathrm{eq}}\downarrow, \qquad k_b\uparrow.} \tag{51}$$

7 Low-Rotation Expansion and Quantitative Signatures

For $|\Omega|$ small compared with $\sigma_0/(\chi\zeta)$, equation (31) gives

$$\sigma(\Omega) = \sigma_0 + \frac{\chi^2\zeta^2}{2\sigma_0}\Omega^2 + O(\Omega^4). \tag{52}$$

Define the dimensionless logarithmic sensitivity

$$\alpha_A \equiv \frac{\sigma_0}{A}\frac{\mathrm{d}A}{\mathrm{d}\sigma}\bigg|_{\sigma_0} > 0. \tag{53}$$

Then

$$\frac{\Delta A}{A_0} = \frac{\alpha_A\chi^2\zeta^2}{2\sigma_0^2}\Omega^2 + O(\Omega^4). \tag{54}$$

The fractional microscopic contraction is

$$\boxed{\frac{\Delta d_{\mathrm{eq}}}{d_0} = -\frac{\alpha_A\chi^2\zeta^2}{2(m-n)\sigma_0^2}\Omega^2 + O(\Omega^4).} \tag{55}$$

The fractional bond stiffening is

$$\boxed{\frac{\Delta k_b}{k_{b0}} = \frac{(m+2)\alpha_A\chi^2\zeta^2}{2(m-n)\sigma_0^2}\Omega^2 + O(\Omega^4).} \tag{56}$$

Both leading signatures are even under reversal of the rotation direction. This is a direct consequence of the parity-even finite-stiffness relation equations (24) and (27).

8 From Microscopic Bonds to an Emergent Rod

8.1 Length of a uniform chain

Consider a one-dimensional chain of N_b identical bonds. Its preferred proper length is

$$L_0(\Omega) = N_b d_{\mathrm{eq}}[\sigma(\Omega)]. \tag{57}$$

Therefore,

$$\frac{\mathrm{d}L_0}{\mathrm{d}|\Omega|} = N_b\frac{\mathrm{d}d_{\mathrm{eq}}}{\mathrm{d}|\Omega|} < 0. \tag{58}$$

The contracting rod is not inserted as an elementary object. It is the coarse-grained equilibrium of a rotation-sensitive network.

8.2 Axial stiffness and effective modulus

For N_b identical bonds in series, the axial spring constant is

$$K_{\text{rod}} = \frac{k_b}{N_b}. \tag{59}$$

If the cross-sectional area is $\mathcal{A}$, the effective Young modulus is

$$Y_{\text{eff}} = \frac{K_{\text{rod}} L_0}{\mathcal{A}} = \frac{k_b d_{\text{eq}}}{\mathcal{A}}. \tag{60}$$

Using equations (43) and (47),

$$Y_{\text{eff}} \propto A^{(m+1)/(m-n)}. \tag{61}$$

Hence

$$\boxed{\frac{\mathrm{d}Y_{\text{eff}}}{\mathrm{d}|\Omega|} > 0.} \tag{62}$$

At low rotation,

$$\frac{\Delta Y_{\text{eff}}}{Y_0} = \frac{(m+1)\alpha_A \chi^2 \zeta^2}{2(m-n)\sigma_0^2}\Omega^2 + O(\Omega^4). \tag{63}$$

Thus the phrase "a very strong rod that is becoming shorter" has a precise effective meaning:

$$L_0'(\Omega) < 0, \qquad Y_{\text{eff}}'(\Omega) > 0. \tag{64}$$

8.3 Finite signal speed and the impossibility of perfect rigidity

Increasing stiffness does not imply infinite rigidity. For a simple lattice with constituent inertial mass μ and spacing d_{eq}, a characteristic longitudinal signal speed scales as

$$c_s^2 \sim \frac{k_b d_{\text{eq}}^2}{\mu}. \tag{65}$$

A relativistically admissible constitutive completion must satisfy

$$\boxed{c_s \leq c.} \tag{66}$$

As the binding stiffens, the associated energy density and effective inertia cannot be ignored. A complete stress-energy tensor must enforce the causal bound, as in relativistic constitutive and elasticity frameworks [9, 8]. The present model predicts increasing finite stiffness, not a perfectly rigid body capable of instantaneous stress transmission.

9 Relation to Established Rotational Couplings

Rotation is already known to couple to internal angular-momentum sectors. The Barnett effect demonstrates rotation-induced magnetization in electronic and nuclear systems [13, 14].

Spin–rotation and helicity–rotation couplings provide further examples in which rotational motion changes an internal or measured phase sector [15, 16]. These established effects do not imply the contraction mechanism proposed here. They establish only the narrower point that a map

$$\text{bulk or observer rotation} \longrightarrow \text{internal state response} \tag{67}$$

is not foreign to known physics.

The present model differs in its constitutive output. It requires the internal response to alter an inter-constituent attractive amplitude and therefore an equilibrium length. No such universal length contraction follows from the Barnett effect or standard spin–rotation coupling. Consequently, the known effects are analogues and calibration channels, not evidence that $A'(\sigma) > 0$ is realized in ordinary solids.

10 Dimensionless Competition Parameter and Illustrative Thresholds

Define the leading microscopic contraction coefficient

$$\Lambda_{\text{micro}} = \frac{\alpha_A}{2(m-n)\Omega_{\text{int}}^2}, \qquad \Omega_{\text{int}} \equiv \frac{\sigma_0}{\chi\zeta}, \tag{68}$$

so that $\varepsilon_{\text{micro}} = -\Lambda_{\text{micro}}\Omega^2 + O(\Omega^4)$. For a slender uniform rod of density ρ_m, Young modulus Y, and half-length R rotating about its centre, elementary linear elasticity gives an average centrifugal axial strain of order

$$\varepsilon_{\text{cf}} \simeq \frac{\rho_m R^2}{3Y}\Omega^2, \qquad \Lambda_{\text{cf}} \simeq \frac{\rho_m R^2}{3Y}. \tag{69}$$

This estimate is geometry dependent but supplies a concrete benchmark. Introduce

$$\boxed{\eta \equiv \frac{\Lambda_{\text{micro}}}{\Lambda_{\text{cf}}} = \frac{3Y\alpha_A}{2(m-n)\rho_m R^2 \Omega_{\text{int}}^2}.} \tag{70}$$

Net leading-order contraction requires $\eta > 1$.

As an explicitly illustrative, non-predictive benchmark, take

$$\rho_m = 1.6 \times 10^3 \ \text{kg m}^{-3}, \quad Y = 1.0 \times 10^{11} \ \text{Pa}, \quad R = 10^{-2} \ \text{m}. \tag{71}$$

Then

$$\Lambda_{\text{cf}} \simeq 5.3 \times 10^{-13} \ \text{s}^2. \tag{72}$$

At $\Omega = 10^4 \ \text{s}^{-1}$, the corresponding conventional strain scale is approximately

$$\varepsilon_{\text{cf}} \sim 5.3 \times 10^{-5}, \tag{73}$$

subject to the actual geometry, anisotropy, support, and stress distribution. For $\alpha_A = 1$ and

$m - n = 6$, equality $\eta = 1$ would require

$$\Omega_{\text{int}} \simeq 4.0 \times 10^5 \text{ s}^{-1}. \tag{74}$$

This number is not assigned to any real material. Its purpose is diagnostic: once a microscopic calculation or experiment bounds Ω_{int} and α_A, the model immediately predicts whether inversion is remotely competitive. Atomic-scale internal frequencies combined with order-unity dimensionless couplings generally make Λ_{micro} extremely small; a measurable effect would therefore require an enhanced collective susceptibility, a soft internal mode, or a near-critical mediator sector.

11 Competition Between Centrifugal Expansion and Microscopic Contraction

The microscopic theorem does not erase the ordinary outward load. The observable deformation is the result of competition between two sectors.

Let the ordinary centrifugal or elastic contribution to the fractional length change be

$$\varepsilon_{\text{cf}} = +\Lambda_{\text{cf}}\Omega^2 + O(\Omega^4), \qquad \Lambda_{\text{cf}} > 0. \tag{75}$$

Let the rotation-induced microscopic contribution from equation (55) be

$$\varepsilon_{\text{micro}} = -\Lambda_{\text{micro}}\Omega^2 + O(\Omega^4), \tag{76}$$

with

$$\Lambda_{\text{micro}} = \frac{\alpha_A \chi^2 \zeta^2}{2(m-n)\sigma_0^2} > 0. \tag{77}$$

Then

$$\boxed{\varepsilon_{\text{net}} = (\Lambda_{\text{cf}} - \Lambda_{\text{micro}})\Omega^2 + O(\Omega^4).} \tag{78}$$

Three regimes follow:

$$\Lambda_{\text{cf}} > \Lambda_{\text{micro}} \quad \Rightarrow \quad \text{net expansion,} \tag{79}$$

$$\Lambda_{\text{cf}} = \Lambda_{\text{micro}} \quad \Rightarrow \quad \text{leading-order cancellation,} \tag{80}$$

$$\Lambda_{\text{cf}} < \Lambda_{\text{micro}} \quad \Rightarrow \quad \text{net contraction.} \tag{81}$$

This is the precise mathematical meaning of an inversion of the usual centrifugal expansion. The reversal is not caused by changing the sign of the centrifugal term. It is caused by adding a stronger negative constitutive response whose magnitude grows with rotation.

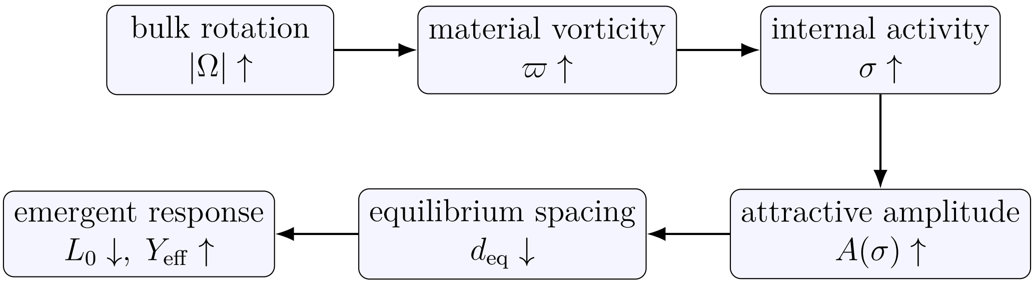

Figure 1: Conditional causal chain of the model. The first and third arrows are model assumptions or constitutive hypotheses; the remaining implications are derived.

12 Closed Ring and Generalized Radial Accommodation

12.1 Rotation-dependent preferred circumference

Let a closed ring contain N_b microscopic bonds. Its preferred summed local comoving circumference is

$$C_0(\Omega) = N_b d_{\mathrm{eq}}[\sigma(\Omega)]. \tag{82}$$

Define the corresponding preferred proper radius

$$\rho_\star(\Omega) \equiv \frac{C_0(\Omega)}{2\pi}. \tag{83}$$

By the microscopic contraction theorem,

$$\rho'_\star(\Omega) \leq 0 \tag{84}$$

for $\Omega \geq 0$, with strict inequality when the coupling is nonzero.

Let r be the laboratory radius and

$$\gamma = \frac{1}{\sqrt{1 - \Omega^2 r^2/c^2}}. \tag{85}$$

The summed local comoving circumference is

$$C_{\mathrm{proper}} = \gamma C_{\mathrm{lab}} = 2\pi\gamma r. \tag{86}$$

12.2 Strong-locking branch

The strong-locking equilibrium condition is

$$C_{\mathrm{proper}} = C_0(\Omega), \tag{87}$$

or

$$\gamma r = \rho_\star(\Omega). \tag{88}$$

Solving self-consistently gives

$$\boxed{r(\Omega) = \frac{\rho_\star(\Omega)}{\sqrt{1+\Omega^2\rho_\star^2(\Omega)/c^2}}.} \tag{89}$$

The associated Lorentz factor and tangential speed are

$$\gamma(\Omega) = \sqrt{1+\frac{\Omega^2\rho_\star^2(\Omega)}{c^2}}, \tag{90}$$

$$v(\Omega) = \frac{\Omega\rho_\star(\Omega)}{\sqrt{1+\Omega^2\rho_\star^2(\Omega)/c^2}} < c. \tag{91}$$

Thus the branch is kinematically subluminal for every finite Ω and finite $\rho_\star$.

Theorem 12.1 (Generalized radial contraction theorem)**.** *Let $\rho_\star(\Omega) > 0$ and $\rho_\star'(\Omega) \leq 0$ for $\Omega \geq 0$. Then the strong-locking laboratory radius equation (89) satisfies*

$$\frac{\mathrm{d}r}{\mathrm{d}\Omega} < 0 \qquad (\Omega > 0). \tag{92}$$

Proof. Differentiating equation (89) gives

$$\frac{\mathrm{d}r}{\mathrm{d}\Omega} = \frac{\rho_\star'(\Omega) - \Omega\rho_\star^3(\Omega)/c^2}{[1+\Omega^2\rho_\star^2(\Omega)/c^2]^{3/2}}. \tag{93}$$

The denominator is positive. For $\Omega > 0$, the second term in the numerator is strictly negative, while the first is nonpositive. Therefore the derivative is strictly negative. □

The theorem contains two contraction channels:

1. the relativistic closure channel represented by the denominator of equation (89);
2. the microscopic binding channel represented by the decrease of $\rho_\star(\Omega)$.

If $\rho_\star$ is constant, the earlier radial-accommodation map is recovered. If $\rho_\star$ decreases, microscopic contraction reinforces the geometric closure effect.

12.3 Ring ordering

For a family of rings labeled by an initial material coordinate ρ, let the preferred proper radius be $\rho_\star(\rho, \Omega)$. If

$$\frac{\partial \rho_\star}{\partial \rho} > 0, \tag{94}$$

then

$$\frac{\partial r}{\partial \rho} = \frac{\partial \rho_\star/\partial \rho}{(1+\Omega^2\rho_\star^2/c^2)^{3/2}} > 0. \tag{95}$$

Thus the rings remain ordered and do not cross on the strong-locking branch.

13 Finite-Stiffness Ring Equilibrium

The exact branch is the infinite-stiffness limit. To study the leading correction, let the circumference energy near its preferred value be

$$U_C = \frac{\kappa_C(\Omega)}{2}\left[C_{\text{proper}} - C_0(\Omega)\right]^2. \tag{96}$$

For N_b identical microscopic bonds in series,

$$\boxed{\kappa_C = \frac{k_b}{N_b}.} \tag{97}$$

Thus the microscopic stiffening theorem directly increases the circumference stiffness.

For a stationary thin ring at externally controlled angular velocity Ω, use the reduced laboratory-time Lagrangian

$$L_r(r;\Omega) = -M_0c^2\sqrt{1-\Omega^2r^2/c^2} - U_C(2\pi\gamma r;\Omega). \tag{98}$$

The stationary condition is

$$M_0\gamma\Omega^2 r = 2\pi\kappa_C\gamma^3\left(C_{\text{proper}} - C_0\right). \tag{99}$$

Therefore

$$C_{\text{proper}} - C_0 = \frac{M_0\Omega^2 r}{2\pi\kappa_C\gamma^2} > 0. \tag{100}$$

Finite stiffness permits a small outward departure from the exact preferred circumference. Let r_0 denote the strong-locking radius. Since

$$\left.\frac{\partial C_{\text{proper}}}{\partial r}\right|_{r_0} = 2\pi\gamma_0^3, \tag{101}$$

the leading radius correction is

$$\boxed{\delta r \simeq \frac{M_0\Omega^2 r_0}{4\pi^2\kappa_C\gamma_0^5} > 0.} \tag{102}$$

This correction competes with the contraction of the preferred radius. As rotation strengthens the microscopic bonds, $\kappa_C(\Omega)$ increases, suppressing the outward correction.

Within this reduced fixed-Ω model, the local strong-locking branch is stable when

$$\boxed{\kappa_C > \frac{M_0\Omega^2}{4\pi^2\gamma_0^3}.} \tag{103}$$

Using equation (97), the condition becomes a microscopic support inequality,

$$k_b > \frac{N_b M_0 \Omega^2}{4\pi^2 \gamma_0^3}. \tag{104}$$

The rotation-induced stiffening can therefore enlarge the stable domain, although the full dynamical stability problem requires radial kinetic terms, phase dynamics, and inter-ring couplings.

14 Relativistic Consistency

14.1 No superluminal material speed

Equation equation (91) gives $v < c$ identically. The generalized contraction does not require a material point to cross the light-speed boundary and remains within the kinematic structure of special relativity [2, 6].

14.2 No instantaneous rigidity

The model permits increasing stiffness but imposes the causal requirement equation (66). A physically complete constitutive law must produce hyperbolic equations with characteristic speeds no greater than c.

14.3 Local covariance of the coupling

The quantities used in equations (25) and (29) are covariant scalars or tensor contractions: $u^\mu \nabla_\mu \Theta$, σ, and $\omega_{\mu\nu}\omega^{\mu\nu}$. No preferred inertial coordinate system is required by the form of the stationary strong-locking sector.

14.4 Energy and angular-momentum accounting

A change in rotation cannot occur without torque. For a driven system,

$$\frac{\mathrm{d}E_{\text{total}}}{\mathrm{d}t} = \tau_{\text{ext}}\Omega - \mathcal{P}_{\text{diss}}, \tag{105}$$

where $\mathcal{P}_{\text{diss}} \geq 0$ represents dissipation. Rotation-dependent binding contributes to both the energy and the torque response. In a conservative completion,

$$J = \frac{\partial L}{\partial \Omega}, \qquad \tau_{\text{ext}} = \frac{\mathrm{d}J}{\mathrm{d}t}. \tag{106}$$

If the binding energy becomes more negative during spin-up, the released energy must appear in kinetic, field, elastic, or dissipative channels. If internal activity requires positive excitation energy, that energy must be supplied by the external work. The effective model does not permit energy creation from nothing; it requires a complete accounting once a microscopic Lagrangian is specified.

14.5 Finite stiffness and the remaining continuum problem

The positive potentials equations (25) and (29) and the reduced Hamiltonian equation (30) provide a bounded homogeneous activity sector and replace the earlier purely multiplier-imposed branch. They establish local stationary stability of the activity minimum. They do not by themselves constitute a complete relativistic continuum theory: the full velocity Hessian, constraint algebra, characteristic cone, and stress-energy tensor must still be derived when Θ, σ, strain, and vorticity are all dynamical. The contraction and stiffness theorems require only the stable stationary branch and therefore do not assume that this larger open problem has already been solved.

15 Internal Attraction, Effective Gravity, and the Missing External Field

The model produces an inward structural response in two related senses.

First, the attractive part of the microscopic pair interaction increases with rotation. This lowers the equilibrium separation and increases the restoring force against displacement.

Second, a rotating ring requires inward stress to maintain circular motion. The emerging network supplies a pathway through which this stress is transmitted.

For material points participating in the structure, one may define an effective inward acceleration

$$g_{\text{eff}} = \Omega^2 r \tag{107}$$

in the nonrelativistic limit, or the corresponding proper acceleration

$$a_{\text{proper}} = \gamma^2 \Omega^2 r \tag{108}$$

for uniform circular motion.

These statements do not yet imply a field acting on an unconnected external test body. To obtain a gravitational theory, one would need at least:

1. a propagating field sourced by the rotating/bound structure;
2. a universal coupling to energy-momentum or to all material clocks and rods;
3. an exterior solution and a force or geodesic law for independent test bodies;
4. agreement with the weak-field inverse-square limit, gravitational redshift, lensing, and other established tests.

The present conclusion is narrower and defensible:

$$\boxed{\begin{array}{c}\text{Rotation-dependent microscopic binding can generate an inward structural}\\ \text{attraction and a contracting support network.}\end{array}} \tag{109}$$

Whether this internal architecture is a precursor, analogue, or microscopic realization of gravity is a separate research question.

16 Microscopic-Observer Thought Experiment Revisited

Imagine observers sufficiently small and sufficiently weakly coupled that they can resolve the internal organization of a macroscopic rod without significantly disturbing it. They would not see a featureless continuum. They would resolve constituents, equilibrium separations, phase rates, propagating stress disturbances, and local binding-energy gradients.

When the rod is spun faster, the two descriptions would be:

$$\text{macroscopic description:} \quad L_0 \downarrow, \quad Y_{\text{eff}} \uparrow, \tag{110}$$

$$\text{microscopic description:} \quad \sigma \uparrow, \quad A \uparrow, \quad d_{\text{eq}} \downarrow, \quad k_b \uparrow . \tag{111}$$

These are not competing realities. They are scale-separated descriptions connected by coarse graining.

The thought experiment is useful because human intuition often grants dynamical reality to astronomical separations while treating microscopic organization as abstract. The observer-scale lemma removes this asymmetry: physical truth does not depend on whether the relevant architecture is visually large or small relative to the observer.

Nevertheless, visual similarity is not enough. An atom and a planetary system need not obey the same equations merely because both can be drawn as a center with surrounding structure. The present model is defined by its phase, vorticity, and binding equations, not by the visual resemblance alone.

17 Thermal, Mechanical, and Electromagnetic Systematics

A rotation-correlated length change is not by itself evidence for the proposed coupling. The measured strain must be decomposed as

$$\varepsilon_{\text{meas}} = \varepsilon_{\text{cf}} + \varepsilon_{\text{micro}} + \alpha_T \Delta T + \varepsilon_{\text{support}} + \varepsilon_{\text{aero}} + \varepsilon_{\text{EM}} + \varepsilon_{\text{plastic}} + \cdots , \tag{112}$$

where α_T is the thermal-expansion coefficient. Frictional or aerodynamic power scales schematically as

$$P_{\mathrm{loss}} = \tau_{\mathrm{loss}}\Omega, \tag{113}$$

and can generate a false Ω^2 signal through heating. A credible experiment therefore requires, at minimum:

1. operation in vacuum or a characterized gas environment;
2. direct, spatially resolved thermometry and active temperature stabilization;
3. measurement below elastic, fatigue, and whirl-instability limits;
4. reversal between $+\Omega$ and $-\Omega$ and comparison with a nonrotating thermal-control specimen;
5. simultaneous measurement of length, resonance frequencies or modulus, and any internal spectral observable;
6. finite-element modelling of support, centrifugal, anisotropic, and gyroscopic stresses.

The parity-even signal proposed here is unchanged under $\Omega \to -\Omega$. Direction-odd signals identify other rotational couplings or apparatus asymmetries, while common even signals must still be separated using thermal and material controls. A particularly useful protocol is a differential pair of nominally identical counter-rotating resonators housed in the same thermal enclosure.

18 Predictions and Falsification Strategy

The hypothesis becomes scientific only when its parameters are connected to measurable quantities. The following observables are direct targets.

18.1 Rotation-dependent length

For a freely responding specimen,

$$\frac{\Delta L}{L} = (\Lambda_{\mathrm{cf}} - \Lambda_{\mathrm{micro}})\,\Omega^2 + O(\Omega^4). \tag{114}$$

A negative coefficient after known thermal, elastic, aerodynamic, and relativistic corrections would be the signature of the proposed inversion.

18.2 Rotation-dependent elastic modulus

The model predicts

$$\frac{\Delta Y}{Y} = \Lambda_Y \Omega^2 + O(\Omega^4), \qquad \Lambda_Y > 0, \tag{115}$$

with Λ_Y related to the contraction coefficient through the exponents m and n.

18.3 Rotation-dependent internal spectral rate

If Θ couples to an observable internal transition, then

$$\Delta\sigma = \frac{\chi^2\zeta^2}{2\sigma_0}\Omega^2 + O(\Omega^4). \tag{116}$$

A spectroscopic or clock comparison could constrain χ. Care is required to separate this proposed proper internal-rate change from ordinary kinematic time dilation, rotational Doppler shifts, magnetic fields, stress shifts, and temperature effects.

18.4 Correlated signature

The strongest test is not one anomalous observable but a correlated set:

$$\Delta L < 0, \qquad \Delta Y > 0, \qquad \Delta\sigma > 0, \tag{117}$$

with the coefficient ratios predicted by one parameter set. A length anomaly without the associated stiffness or internal-rate response would disfavor the model.

18.5 Null result

If precision experiments establish bounds

$$|\Lambda_{\text{micro}}| < \Lambda_{\text{max}} \tag{118}$$

far below the value required to compete with ordinary centrifugal expansion, then the proposed mechanism cannot explain macroscopic contraction in that material. The model is therefore falsifiable at the level of its effective coefficients even before a fundamental microscopic derivation is available.

19 What the Model Establishes

The model establishes the following conditional results.

1. A covariant scalar relation can couple the magnitude of material vorticity to a comoving internal activity rate without violating the light-speed limit at the kinematic level.
2. For the specified repulsive-attractive pair potential, an attractive amplitude increasing with internal activity produces a monotonically decreasing equilibrium separation.
3. The same assumptions produce a monotonically increasing microscopic stiffness and coarse-grained elastic modulus.
4. A chain of such bonds has a preferred proper length that decreases with rotation and therefore constitutes an emergent contracting rod.

5. A closed ring built from the bonds has a rotation-dependent preferred proper circumference. In the strong-locking limit, this produces the exact generalized radial map equation (89).
6. If the preferred proper radius is nonincreasing, the laboratory radius decreases monotonically and the tangential speed remains below c.
7. Finite microscopic stiffness gives an outward correction, while rotation-induced stiffening suppresses that correction and can improve the reduced local stability bound.

20 What the Model Does Not Yet Establish

The present work does not establish:

1. that ordinary electrons execute classical planetary orbits;
2. that all atomic or condensed-matter systems possess the internal phase variable and vorticity coupling proposed here;
3. that the mediator toy model or the sign domain in equation (38) is realized by a specified ordinary material or follows from the Standard Model;
4. a complete relativistic continuum stress-energy tensor for a three-dimensional rotating body;
5. global nonlinear stability during spin-up;
6. a complete relativistic continuum Hamiltonian for the coupled phase, activity, strain, and vorticity sectors;
7. a universal external gravitational field acting on bodies not connected to the material network;
8. observational confirmation of rotation-induced microscopic contraction.

A real rotating material may still expand, shear, heat, plastically deform, crack, or fail. The net sign follows from the competition expressed in equation (78), not from rotation alone.

21 Research Program

The next steps are mathematically well defined.

21.1 Microscopic derivation of the attractive amplitude

Use the mediator construction of equations (33) and (37) as a template, identify a concrete electronic, magnetic, phononic, or collective mediator in a specified material, and calculate $A(\sigma)$ and its magnitude from independently measurable parameters.

21.2 Finite-stiffness temporal completion

Promote the bounded homogeneous sector to a covariant continuum action, calculate the full velocity Hessian and characteristic matrix, perform a Dirac–Bergmann or equivalent Hamiltonian analysis, and determine the conserved phase charge and causal domain.

21.3 Continuum constitutive theory

Derive an energy density

$$\epsilon = \epsilon(n, s_{AB}, \Theta, \nabla\Theta, \varpi, \ldots) \tag{119}$$

and the stress-energy tensor

$$T^{\mu\nu} = -\frac{2}{\sqrt{-g}}\frac{\delta S}{\delta g_{\mu\nu}}. \tag{120}$$

Then solve

$$\nabla_\mu T^{\mu\nu} = f^\nu_{\text{ext}} \tag{121}$$

for driven systems and $\nabla_\mu T^{\mu\nu} = 0$ for isolated systems.

21.4 Global stability and spin-up

Study radial, longitudinal, azimuthal, shear, and phase perturbations during finite-time spin-up. Determine whether the contracting branch is dynamically reachable without crossing a loss-of-hyperbolicity or negative-energy boundary.

21.5 Laboratory bounds

Design differential experiments with counter-rotating samples, high-stability cavities, resonant ultrasound, diffraction-based lattice-spacing measurements, and internal clock transitions. The parity-even model predicts the same leading effect for $+\Omega$ and $-\Omega$, while many systematic effects change sign or orientation.

21.6 External-field extension

Only after the internal structural model is completed should one ask whether a propagating field sourced by the phase-stress sector can reproduce an exterior gravitational response. This requires a separate action, source law, exterior solution, and comparison with gravitational tests.

22 Conclusion

The rod and spinning-top thought experiment originally separates the geometry of circular motion from the mechanism that produces it. A gravitational field and a mechanical constraint can supply related radial accelerations while remaining physically distinct. The present work reverses the explanatory direction and asks how the constraint itself could emerge.

A covariant strong-locking model was introduced in which material vorticity increases an internal activity rate. A general microscopic pair potential was then considered whose attractive amplitude increases with that rate. Under explicit assumptions, two results were proved: the equilibrium separation decreases with rotation, and the local stiffness increases. Coarse graining converts these microscopic results into a rod whose preferred length decreases while its elastic modulus increases.

For a closed ring, the preferred proper circumference becomes rotation dependent. Combining microscopic contraction with relativistic circumference closure yields

$$r(\Omega) = \frac{\rho_\star(\Omega)}{\sqrt{1+\Omega^2\rho_\star^2(\Omega)/c^2}}.$$

This map is monotonically contracting when $\rho_\star'(\Omega) \le 0$, preserves ring ordering under a monotonic material map, and keeps the tangential speed subluminal.

The key physical conclusion is therefore conditional but precise:

> If bulk rotation increases a microscopic internal activity, and if that activity strengthens the attractive part of the constituent binding, then increasing rotation makes the preferred material structure shorter and stiffer. When the microscopic contraction exceeds ordinary centrifugal expansion, the net macroscopic deformation reverses sign. (122)

The observer's size does not determine whether this architecture is physically real. It determines whether the architecture is resolved as a microscopic network or represented as a continuous rod. The unresolved question is empirical and dynamical, not logical: does real matter possess the proposed coupling with sufficient strength, and can the constrained sector be completed as a healthy relativistic field theory?

A Detailed Derivation of the Pair Equilibrium

Starting from

$$U = Bd_\star^m d^{-m} - Ad_\star^n d^{-n}, \tag{123}$$

one obtains

$$U_d = -mBd_\star^m d^{-m-1} + nAd_\star^n d^{-n-1}. \tag{124}$$

The equilibrium relation is

$$mBd_\star^m d_{\mathrm{eq}}^{-m-1} = nAd_\star^n d_{\mathrm{eq}}^{-n-1}, \tag{125}$$

which gives equation (43).

The second derivative is

$$U_{dd} = m(m+1)Bd_\star^m d^{-m-2} - n(n+1)Ad_\star^n d^{-n-2}. \tag{126}$$

At equilibrium,

$$m(m+1)Bd_\star^m d_{\mathrm{eq}}^{-m-2} = n(m+1)Ad_\star^n d_{\mathrm{eq}}^{-n-2}. \tag{127}$$

Hence

$$k_b = n(m-n)Ad_\star^n d_{\mathrm{eq}}^{-n-2} > 0. \tag{128}$$

Substitution of equation (43) yields equation (47).

B Derivation of the Generalized Radial Map

From

$$\gamma r = \rho_\star, \qquad \gamma = (1 - \Omega^2 r^2/c^2)^{-1/2}, \tag{129}$$

we have

$$\frac{r^2}{1 - \Omega^2 r^2/c^2} = \rho_\star^2. \tag{130}$$

Therefore

$$r^2\left(1 + \frac{\Omega^2\rho_\star^2}{c^2}\right) = \rho_\star^2, \tag{131}$$

and the positive-radius solution is equation (89).

The derivative with respect to $\rho_\star$ at fixed Ω is

$$\frac{\partial r}{\partial \rho_\star} = \left(1 + \Omega^2\rho_\star^2/c^2\right)^{-3/2} > 0, \tag{132}$$

which produces equation (95) by the chain rule.

C Low-Rotation Coefficient Relations

Define

$$Q \equiv \frac{\alpha_A \chi^2 \zeta^2}{2\sigma_0^2}. \tag{133}$$

Then the leading microscopic predictions are

$$\frac{\Delta A}{A_0} = Q\Omega^2 + O(\Omega^4), \tag{134}$$

$$\frac{\Delta d}{d_0} = -\frac{Q}{m-n}\Omega^2 + O(\Omega^4), \tag{135}$$

$$\frac{\Delta k_b}{k_{b0}} = \frac{m+2}{m-n}Q\Omega^2 + O(\Omega^4), \tag{136}$$

$$\frac{\Delta Y}{Y_0} = \frac{m+1}{m-n}Q\Omega^2 + O(\Omega^4). \tag{137}$$

Eliminating Q gives parameter-independent coefficient ratios within the pair-potential model:

$$\frac{\Delta k_b/k_{b0}}{-\Delta d/d_0} = m + 2, \tag{138}$$

$$\frac{\Delta Y/Y_0}{-\Delta d/d_0} = m + 1. \tag{139}$$

These correlated ratios provide a stronger falsification target than any single coefficient.

D A Minimal Stationary Effective Action

A schematic covariant stationary action containing the sectors used in the paper is

$$S = \int \sqrt{-g}\, \mathcal{L}\, \mathrm{d}^4 x, \tag{140}$$

with

$$\begin{aligned} \mathcal{L} = & -\epsilon_{\mathrm{mat}}(n, s_{AB}) - n_b U(d, \sigma) - \frac{K_s}{2}\left(h^{\mu\nu}\nabla_\mu\phi\nabla_\nu\phi - q_0^2\right)^2 \\ & - \frac{K_\Theta}{2}(u^\mu\nabla_\mu\Theta - \sigma)^2 - \frac{K_\sigma}{4}(\sigma^2 - \sigma_0^2 - \chi^2\varpi^2)^2 - \frac{Z_\sigma}{2}h^{\mu\nu}\nabla_\mu\sigma\nabla_\nu\sigma, \end{aligned} \tag{141}$$

where n_b is a bond-density variable, s_{AB} denotes material strain variables, and ϕ is an optional spatial winding phase responsible for circumference locking. The positive coefficients $K_\Theta, K_\sigma, Z_\sigma$ define a finite stationary locking sector. Its large-stiffness branch reproduces equation (27), while variation with respect to material variables produces the binding and stress response.

Equation equation (141) is intentionally schematic. A predictive continuum theory must define d covariantly through material coordinates or invariants of the strain tensor, derive every coefficient, and calculate the complete stress-energy tensor. It is included to demonstrate that the stationary ingredients can be organized as local covariant scalars rather than as coordinate-specific rules.

References

[1] I. Newton, *Philosophiæ Naturalis Principia Mathematica*, London, 1687.

[2] A. Einstein, "Zur Elektrodynamik bewegter Körper," *Annalen der Physik* **17**, 891–921 (1905).

[3] M. Born, "Die Theorie des starren Elektrons in der Kinematik des Relativitätsprinzips," *Annalen der Physik* **335**, 1–56 (1909).

[4] P. Ehrenfest, "Gleichförmige Rotation starrer Körper und Relativitätstheorie," *Physikalische Zeitschrift* **10**, 918 (1909).

[5] F. Noether, "Zur Kinematik des starren Körpers in der Relativtheorie," *Annalen der Physik* (1910).

[6] W. Rindler, *Relativity: Special, General, and Cosmological*, 2nd ed., Oxford University Press, 2006.

[7] L. D. Landau and E. M. Lifshitz, *The Classical Theory of Fields*, 4th ed., Butterworth-Heinemann, 1975.

[8] L. D. Landau and E. M. Lifshitz, *Theory of Elasticity*, 3rd ed., Butterworth-Heinemann, 1986.

[9] R. Beig and B. G. Schmidt, "Relativistic elasticity," *Classical and Quantum Gravity* **20**, 889–904 (2003).

[10] Ø. Grøn, "Relativistic description of a rotating disk," *American Journal of Physics* **43**, 869 (1975).

[11] S. M. H. Emamifar, "Radial Accommodation in the Ehrenfest Problem: A Conditional Layered-Ring Model with an Effective Covariant Phase-Stiffness Realization," unpublished manuscript, IRCBHC (2026).

[12] S. M. H. Emamifar, "The Rod and the Spinning Top Thought Experiment: Reproducing Orbital-Like Kinematics Without Gravity," unpublished manuscript, IRCBHC (2026).

[13] S. J. Barnett, "The Magnetization of Iron, Nickel, and Cobalt by Rotation and the Nature of the Magnetic Molecule," *Proceedings of the National Academy of Sciences* **3**, 178–181 (1917), doi:10.1073/pnas.3.3.178.

[14] M. Arabgol and T. Sleator, "Observation of the Nuclear Barnett Effect," *Physical Review Letters* **122**, 177202 (2019), doi:10.1103/PhysRevLett.122.177202.

[15] B. Mashhoon, R. Neutze, M. Hannam, and G. E. Stedman, "Observable frequency shifts via spin–rotation coupling," *Physics Letters A* **249**, 161–166 (1998).

[16] B. Mashhoon and Y. N. Obukhov, "Spin-of-light gyroscope and the spin–rotation coupling," *Physical Review D* **110**, 104015 (2024), doi:10.1103/PhysRevD.110.104015.

Author Note

This manuscript develops a conditional finite-stiffness effective model. The contraction and stiffening results are exact consequences of the stated assumptions; the mediator toy model demonstrates one stable route to the required sign of the induced attraction, but its realization and magnitude in physical matter remain hypotheses to be tested. The distinction between internal structural attraction and an external gravitational field is maintained throughout.